Thin Solid Films 517 (2009) 6034–6037

Contents lists available at ScienceDirect

Thin Solid Films

journal homepage: www.elsevier.com/locate/tsf

Single layer and multilayered films of plasma polymers analyzed by nanoindentation and spectroscopic ellipsometry

V. Cech *, B. Cechalova, R. Trivedi, J. Studynka

Institute of Materials Chemistry, Brno University of Technology, Purkynova 118, Brno 612 00, Czech Republic

ARTICLE INFO

Article history:
Received 18 December 2008
Received in revised form 8 May 2009
Accepted 14 May 2009
Available online 22 May 2009

Keywords:
Multilayers
Plasma processing and deposition
Ellipsometry
Atomic force microscopy (AFM)

ABSTRACT

Well-defined single layer and multilayered a-SiC:H films, deposited from tetravinylsilane at different powers by plasma-enhanced chemical vapor deposition on silicon, were intensively studied by in situ spectroscopic ellipsometry, nanoindentation, and atomic force microscopy. A realistic model of the sample structure was used to analyze ellipsometric data and distinguish individual layers in the multilayered film, evaluate their thickness and optical constants. Dispersion dependences for the refractive index were well separated for each type of individual layer, if the thickness was decreased from 315 to 25 nm, and corresponded to those of the single layer. A beveled section of the multilayered film revealed the individual layers that were investigated by atomic force microscopy and nanoindentation to confirm that mechanical properties in multilayered and single layer films are similar.

1. Introduction

Plasma polymer films in the form of hydrogenated amorphous carbon-silicon (a-SiC:H) or carbon-silicon oxide (a-SiOC:H) alloy are often used as barrier or protective layers for polymer and metal substrates, cutting tools, electronic, and optoelectronic devices. Properties of the devices are influenced by interfacial phenomena. To eliminate or at least reduce the internal stresses and improve adhesion, mostly multilayered rather than a single layer film has to be used. Such multilayers may be used for passivation of organic devices [1], as a dielectric barrier in semiconductor devices [2], as tribological coatings in aeronautical applications [3], or as a functional coating in polymer composites with controlled interphases [4].

The performance of fiber-reinforced composites (FRC) is strongly influenced by the functionality of the composite interphase [5]. The functional coating (interlayer) therefore has to be tailored [6] to improve the transfer of stress from the polymer matrix to the fiber reinforcement by enhancing fiber wettability, adhesion, compatibility, etc. A single interlayer seems not to be sufficiently suitable for high performance FRC due to material differences at the interfaces of quite distinct materials. The Young's modulus of the fibre (73 GPa for glass fibre) differs from that of the polymer matrix (4 GPa for polyester resin) by one order or more, for example. The physical and chemical incompatibility of both the phases results in high-stress concentrations under both mechanical and thermal loading [7]. For this reason, a functional multilayer, comprising individual layers of gradually changed physical and chemical properties, could be used to improve compatibility within the composite interphase. The fibre-coating method for toughening composites seems to be one of the most effective methods for achieving simultaneous high strength and high toughness when an appropriate interlayer material is chosen [8].

Bilayers consisting of a-SiC:H and a-SiOC:H alloys were deposited using plasma-enhanced chemical vapor deposition (PECVD). The layered structures were subjected to ellipsometric measurements that enabled us to distinguish individual layers and determine the layer thickness and its optical constants [9]. The thickness of individual layers varied from 0.1 to 1 μm. The refractive index of both the alloys differed by 0.15 (633 nm) and thus the difference was relatively high due to the combination of alloys with and without oxygen.

In this study, single layer and multilayered a-SiC:H films, deposited from tetravinylsilane (TVS) at different powers by PE CVD on silicon, were investigated intensively by spectroscopic ellipsometry, nanoindentation, and atomic force microscopy (AFM) to compare optical and mechanical properties of the individual layer of decreased thickness (315–25 nm) with those of the corresponding single layer. A vinyl group is intended for chemical bonding with polymer matrix in FRC.

2. Experimental details

Plasma-polymerized tetravinylsilane films were deposited on single-side polished silicon wafers using PECVD (13.56 MHz) working in a pulsed regime. The effective power (W_{eff}) of the pulsed plasma was controlled by changing the ratio of the time when the plasma was switched on (t_{on} = 1 ms) to the time when it was switched off (t_{off} = 4–499 ms) at a total power of 50 W (W_{total}), i.e., $W_{eff} = t_{on} / (t_{on} + t_{off}) \times W_{total}$. The effective power therefore varied from 0.1 to 10 W. The silicon wafer was pretreated with O_2 plasma (5 sccm, 4 Pa, 25 W) for 10 min. Single layers and multilayers of a-SiC:H were deposited at a flow rate of 0.50 sccm and a corresponding pressure of 1.3 Pa using TVS plasma. The multilayer was hidden in the load lock, while the different power was set up to deposit

* Corresponding author. Tel.: +420 541 149 304; fax: +420 541 149 361.
E-mail address: cech@fch.vutbr.cz (V. Cech).

0040-6090/$ – see front matter © 2009 Elsevier B.V. All rights reserved.
doi:10.1016/j.tsf.2009.05.025

the next individual layer. Deposited films were held for 1 h in argon gas (10 sccm, 10 Pa) and then moved to the load lock and flushed with air to atmospheric pressure.

In situ spectroscopic ellipsometry was employed as the non-destructive technique to evaluate the single layer or multilayered film. The technique allows investigation of thicknesses of individual layers and their optical parameters, such as the refractive index and extinction coefficient. Deposited films were studied using a phase-modulated spectroscopic ellipsometer UVISEL (Jobin-Yvon) working in the region of 240–830 nm. The dispersion dependence of the dielectric function was fitted using the five-parametric Tauc–Lorentz formula [10]. According to this model, the imaginary part of the dielectric function e_2 is obtained by multiplying the Tauc joint density of states $(E-E_g)^2/E^2$ by the expression for e_2 obtained from the Lorentz oscillator model

$$\varepsilon_2(E) = \begin{cases} \dfrac{E_0}{E} \cdot \dfrac{A \cdot \Gamma \cdot \left(E-E_g\right)^2}{\left(E^2-E_0^2\right)^2 + \Gamma^2 \cdot E^2} & E > E_g \\ 0 & E \le E_g \end{cases}, \quad (1)$$

where E_g is the optical band gap, E_0 the peak transition energy, Γ the broadening term, and A the product of the oscillator amplitude and Tauc constant. The real part of the dielectric function e_1 is calculated from the Kramers–Kronig relation

$$\varepsilon_1(E) = \varepsilon_1(\infty) + \frac{2}{\pi} \cdot P \int_{E_g}^{\infty} \frac{\chi \cdot \varepsilon_2(\xi)}{\chi^2 - E^2} \mathrm{d}\chi, \quad (2)$$

where P is the Cauchy principal part of the integral with the inclusion of an additional fitting parameter $e_1(\infty)$.

Mechanical properties of the plasma polymer films were investigated very precisely using a nanoindentation technique. The Young's modulus and the hardness of the films were determined according to the Oliver and Pharr method [11] from load–displacement curves obtained using an TS 70 TriboScope (Hysitron) attached to an NTegra Prima Scanning Probe Microscope (NT-MDT), equipped with a three-sided pyramid Berkovich indenter. Measured data were obtained from one complete cycle of loading and unloading, where the loading and unloading rate was in the range of 3–20 μN s^{-1} with a minimum load of 1 μN and a hold time of 5 s. The unloading data were then analyzed according to the equation

$$S = \frac{2}{\sqrt{\pi}} E_r \sqrt{A}, \quad (3)$$

where the experimentally measured stiffness S was determined as a slope ($S = \mathrm{d}P/\mathrm{d}h$, P is the applied force, h is the displacement) of the upper portion of the unloading curve. A is the projected area of the elastic contact and E_r is the reduced modulus defined by the equation

$$\frac{1}{E_r} = \frac{\left(1-\nu^2\right)}{E} + \frac{\left(1-\nu_i^2\right)}{E_i}, \quad (4)$$

where E and ν are the Young's modulus and Poisson's ratio for the specimen, and E_i and ν_i are the same parameters for the Berkovich indenter, with $E_i = 1141$ GPa and $\nu_i = 0.07$. The Poisson's ratio, ν, used in Eq. (4) was 0.5 for all samples. The hardness is determined from measured data using the equation

$$H = \frac{P_{max}}{A}, \quad (5)$$

where P_{max} is the maximum applied force.

3. Results and discussion

Some theoretical and experimental studies have shown that the coated material should be ductile or flexible with the interlayer modulus close to that of the polymer matrix [7]. In order to decrease the degree of cross-linking of plasma polymer, we reduced the effective power (10–0.1 W) using pulsed plasma, resulting in a material of lower Young's modulus. Monomer molecules are more activated and fragmented forming a higher density of free radicals if the plasma energy (power) increases, and the reactive species result in a highly cross-linked polymer. A cross-linking of the material may also be supported by ion bombardment. It has been shown that the ion energy effectively enhances the film packing density [12].

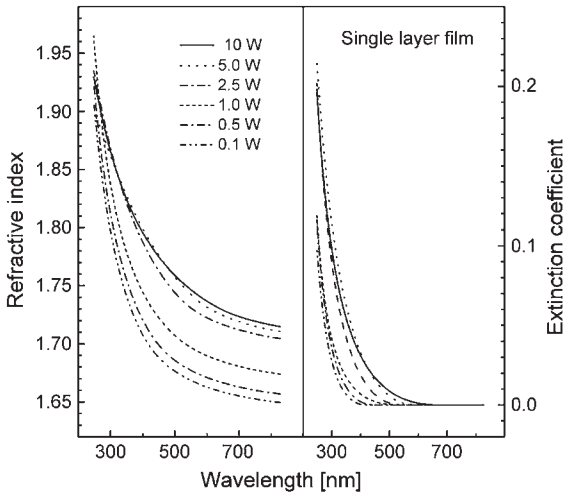

Fig. 1. Dispersion dependences for the refractive index and extinction coefficient of single layer a-SiC:H film deposited at different powers.

Single layer films of about 1 μm thickness were deposited at powers of 0.1, 0.5, 1.0, 2.5, 5.0, and 10 W. The flow rate of TVS monomer was constant (0.50 sccm). Deposited films were evaluated by spectroscopic ellipsometry and nanoindentation. Optical characterization of the films requires not only appropriate parameterization of the material optical constants but also a realistic model of the sample structure. Our model consisted of a semi-infinite substrate (crystalline silicon together with a silicon dioxide layer), a plasma polymer layer, and a surface overlayer (OL) corresponding to the surface roughness of the film [13]. The overlayer was modeled as the effective medium [14] with a fixed ratio (50%) of the plasma polymer and air. An interlayer between the plasma polymer layer and the substrate was not confirmed by modeling. Ellipsometric data obtained for pretreated silicon wafers enabled us to evaluate the thickness of the silicon dioxide layer at the surface of the wafer; the value was 4.1 nm. This parameter was fixed for the sample model in the bilayer form $Si–SiO_2$/layer/OL. Dispersion curves for the refractive index and the extinction coefficient corresponding to the single layer films are shown in Fig. 1. The refractive index increased from 1.66 (0.1 W) to 1.73 (10 W) at a wavelength of 633 nm with enhanced effective power. A shift of the UV absorption edge towards longer wavelengths (413 nm at 0.1 W and 653 nm at 10 W) was evident for enhanced power.

The Young's modulus and hardness of the single layer films were determined from nanoindentation measurements performed at a penetration depth of 10% of the film thickness, i.e., about 0.1 μm. The mechanical constants and the refractive index are plotted as a function of the effective power in Fig. 2. An increasing trend of mechanical constants with enhanced power is similar to that for the refractive index. The Young's modulus (hardness) increased from 9.6 (0.9) to 26 GPa (4.5 GPa), respectively. However, the Young's modulus rose by 170% and the hardness by 400%, while the refractive index increased only 4% (633 nm). Thus, the mechanical properties of a-SiC:H alloy were more sensitive to the power used for deposition of the material. On the basis of previous chemical analyses (X-ray photoelectron spectroscopy, Rutherford backscattering spectrometry, elastic recoil detection analysis, Fourier transform infrared spectroscopy) [15], we know that the organic/inorganic character of the a-SiC:H alloy, expressed by the C/Si

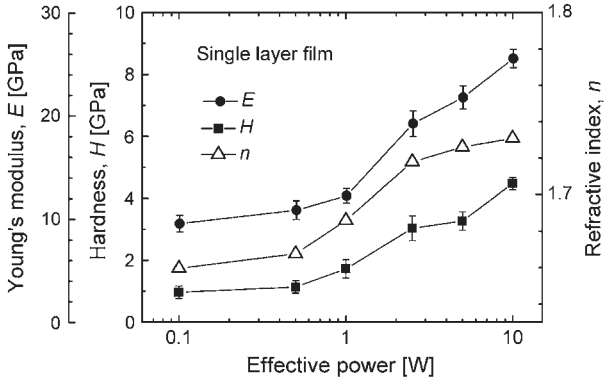

Fig. 2. Young's modulus, hardness, and refractive index (633 nm) of single layer a-SiC:H film as a function of the effective power.

ratio, varied from 3 to 8 with increased power. The a-SiC:H alloy deposited at 0.1 W (Si: 9 at.%, C: 35 at.%, H: 56 at.%) was formed mostly of a carbon network with a smaller proportion of Si–C bonding species and the vinyl as side groups. However, the proportion of Si–C bonding species and vinyl groups decreased with enhanced power (Si: 5 at.%, C: 40 at.%, H: 55 at.% at 10 W) [15]. We could expect that the enhanced mechanical constants resulted from both a higher cross-linking of the plasma polymer and a higher proportion of stronger C–C bonding species (348 kJ/mol) rather than Si–C (290 kJ/mol) [16]. The increased density of polarizable species may dominate the structure changes in a-SiC:H alloy and, in accordance with the Clausius–Mossotti relationship [17], the refractive index increased slightly with enhanced power.

A functional multilayer may be used to control the composite interphase, where the thickness and mechanical constants of the individual layers are the key parameters. For this purpose, in situ spectroscopic-ellipsometry monitoring of multilayer growth during the deposition process would be helpful. Two a-SiC:H alloys of distinct optical properties were chosen to construct a multilayer: layer A was deposited at 10 W and layer B at 0.1 W. Multilayered a-SiC:H films consisting of ten layers were constructed from layers A and B using a layer-by-layer rotating system. Layer B was deposited as the first layer on the silicon substrate; layer A was the last layer at the surface of the layered structure. Four samples of ten-layered a-SiC:H films were deposited, changing the layer thickness from about 70 to 300 nm on the basis of the mean deposition rate (120 nm/min for layer A, 16.5 nm/min for layer B) evaluated from the growth of the single layer.

Ellipsometric data were analyzed using the sample model in the 11-layer form Si–SiO_2/BABABABABA/OL. The dispersion dependence of the dielectric function was fitted using the five-parametric Tauc–Lorentz formula and starting from optical constants determined for the single layer film. An extended model including the gradient interlayer (mixing layers at the interface between the layers A and B) resulted in a negligible interlayer thickness; thus, we expect a relatively sharp interface between the individual layers. Ellipsometric measurements enabled us to distinguish individual layers in the multilayered film and evaluate their thickness and optical constants (refractive index, extinction coefficient). Dispersion dependences for the optical constants corresponding to layers A and B of all the samples are given in Fig. 3. The dispersion curves for the refractive index are well separated into two groups (except the UV range, where absorption of layers increased) according to the layer type — A or B — and their plots correspond to those for the single layer film. The dispersion curves for the extinction coefficient of layers A and B are mostly sorted, but the differences are relatively small. Sample 1 was fabricated as a 2-μm-thick structure comprising layer A of thickness 100 ± 19 nm and layer B (315 ± 12 nm), respectively. The total thickness of samples 2 and 3 was 1 μm; the thickness of layer A was 120 ± 5 nm (sample 2) and 122 ± 6 nm (sample 3), and the thickness of layer B was 96 ± 9 nm (sample 2) and 69 ± 7 nm (sample 3). Sample 4 had a modified configuration: a buffer

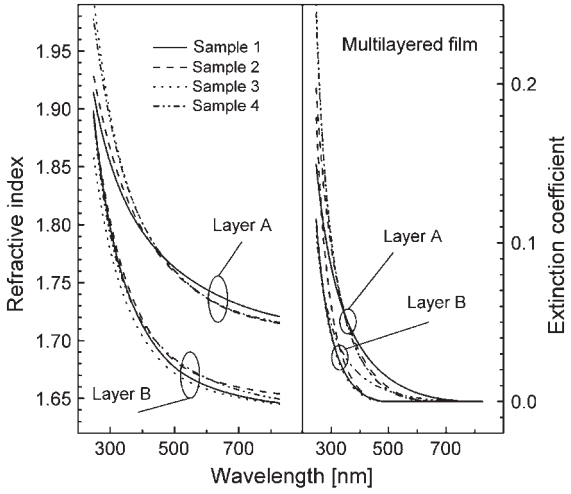

Fig. 3. Dispersion dependences for the refractive index and extinction coefficient of ten-layered a-SiC:H films comprising layers A and B. Description of samples is given in the text.

layer A of 1-μm thickness was deposited on silicon substrate before the formation of a 10-layer stack. A layer A of thickness 129 ± 4 nm and a layer B of thickness 132 ± 5 nm constituted the multilayer. The overlayer thickness was 6–7 nm for all the samples.

Samples 5 and 6 were constructed as trilayered a-SiC:H films, comprising layer B (0.1 W), layer C (1.0 W), and layer A (10 W) from bottom to top. The sample model in the four-layer form Si–SiO_2/BCA/OL was used to analyze the ellipsometric spectra, with the results shown in Fig. 4. We were able to distinguish the individual layers in the multilayered film even if their optical constants were very similar. Dispersion dependences for the refractive index are well detached, as evident from Fig. 4, but those for the extinction coefficient are mixed together. The determined thicknesses of the individual layers (from bottom to top) and the overlayer were 141, 82, 99, and 4 nm for sample 5, and 27, 41, 25, and 3 nm for sample 6.

As the dispersion of the refractive index of the individual layers in multilayered a-SiC:H films corresponded well to that of the single layer film and as the refractive index was well correlated with mechanical constants (Fig. 2), we could expect that the mechanical constants of the individual layers are similar to that of the single layer film. This assumption could be applied only on a basis of the same monomer used at given deposition condition. However, the mechanical constants of

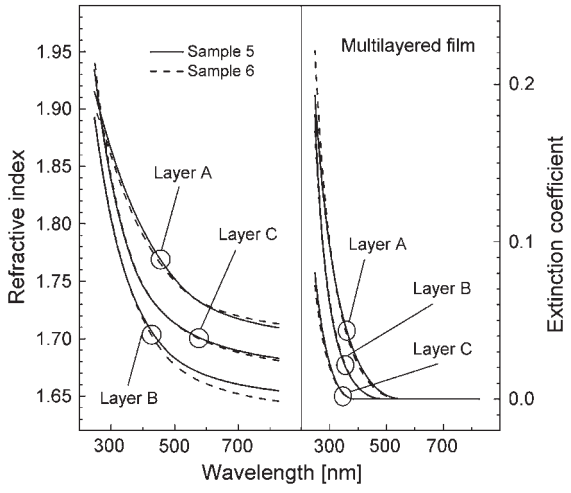

Fig. 4. Dispersion dependences for the refractive index and extinction coefficient of trilayered a-SiC:H films comprising layers A, B, and C. Description of samples is given in the text.

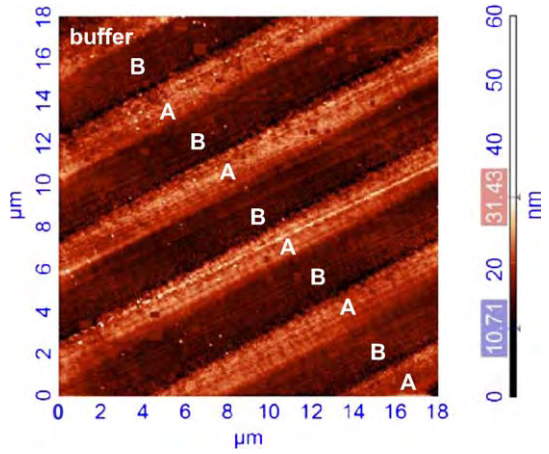

Fig. 5. AFM surface morphology (scan area: $18 \times 18\ \mu m^2$) of sectioned ten-layered a-SiC:H film with buffer layer. Labels for layers A, B and the buffer layer are provided.

individual layers cannot be determined from nanoindentation measurements in the normal direction to the surface of multilayered film because of the influence of the bottom layers and substrate. Any indentation will result in some influence from all the individual layers since the elastic deflections of all the layers contribute to support the indenter load. Sample 4 was used to section the ten-layered a-SiC:H film from the film surface at a small angle of 4° using a Leica EM UC6 ultramicrotome. A 1-µm-thick buffer layer was used in order not to damage the diamond knife due to a contact with the silicon substrate. The uncovered multilayer was observed by AFM (NTegra Prima, NT-MDT) and the surface morphology enabled us to distinguish individual layers in the multilayer (Fig. 5). Ten individual layers could be differentiated from the bottom right corner to the upper left corner, where the buffer layer is visible. The surface morphology of sectioned multilayered film corresponded to stiffness of the individual layer; the individual layer of higher modulus was up (light stripe) while that of lower modulus was down (dark stripe), see Fig. 5. The width of sectioned individual layer increased up to almost 2 µm using a small angle of 4°.

Nanoindentation measurements were made for each uncovered individual layer in the section area; the mean values for layer A were $E = (18.9 \pm 1.0)$ GPa, $H = (2.7 \pm 0.6)$ GPa and those for layer B were $E = (12.7 \pm 1.3)$ GPa, $H = (1.8 \pm 0.5)$ GPa, which are similar to those for the single layer film. The penetration depth was only about 40 nm.

4. Conclusion

Single layer and multilayered a-SiC:H films were deposited on silicon from tetravinylsilane using PECVD. The multilayered films were constructed as a trilayered film, Si–SiO_2/BCA, or as a 10-layered film, Si–SiO_2/BABABABABA, where Si–SiO_2 means a substrate of the silicon together with a silicon dioxide layer. Layer A was deposited at an effective power of 10 W, layer B at 0.1 W, and layer C at 1.0 W, with a constant TVS flow rate (0.50 sccm). Sample models used for analyses of ellipsometric data included an overlayer corresponding to the surface roughness of the film. The ellipsometric analyses enabled us to distinguish individual layers in the multilayered film, because of the sharp interfaces between them, and evaluate their thicknesses and optical constants. Dispersion dependences for the refractive index were well separated although the difference was 0.07 (633 nm) for layers A and B in ten-layered films and only 0.04 (633 nm) in trilayered films using layers A, B, and C. The results evidenced a high reproducibility of the deposition process. Dispersion dependences for the refractive index in the single layer and multilayered films corresponded each other for decreasing thickness of the individual layer 315–25 nm. Thus, correlation between the refractive index and mechanical properties (Fig. 2) indicated similar mechanical properties in the single layer and multilayered films. The assumption was confirmed by nanoindentation measurements: The ten-layered a-SiC:H film was sectioned using ultramicrotomy to reveal the individual layers, which were observed by atomic force microscopy due to the surface morphology influenced by layer stiffness. The distinguished individual layers were investigated by nanoindentation to evaluate the mechanical constants. We expect that optical and mechanical properties of individual layer are a function of the effective power but are independent of number of layers in multilayer system if the thickness of individual layer is >25 nm and thus an influence of interfacial phenomena between the layers can be neglected. The results enable us construction of functional multilayered films of controlled mechanical properties applicable in polymer composites with controlled interphases.

Acknowledgements

This work was supported in part by the Academy of Sciences of the Czech Republic, grant no. KAN101120701, the Czech Science Foundation, grant no. 104/06/0437, and the Czech Ministry of Education, grant no. MSM0021630501. The authors would like to thank Dr. Robert Ranner (Leica Microsystems) for processing of samples.

References

[1] J.H. Lee, C.H. Jeong, J.T. Lim, V.A. Zavaleyev, S.J. Kyung, G.Y. Yeom, Jpn. J. Appl. Phys. 45 (2006) 8430.
[2] Z. Zhang, T. Wagner, W. Sigle, A. Schulz, J. Mater. Res. 21 (2006) 608.
[3] M. Joinet, S. Pouliquen, L. Thomas, F. Teyssandier, D. Aliaga, Surf. Coat. Technol. 202 (2008) 2252.
[4] V. Cech, IEEE Trans. Plasma Sci. 34 (2006) 1148.
[5] J.-K. Kim, Y.-W. Mai, Engineered Interfaces in Fiber Reinforced Composites, Elsevier, Amsterdam, 1998.
[6] L.T. Drzal, M.J. Rich, P.F. Lloyd, J. Adhes. 16 (1983) 1.
[7] M. Labronici, H. Ishida, Compos. Interfaces 2 (1994) 199.
[8] J.-K. Kim, Y.-W. Mai, Compos. Sci. Technol. 41 (1991) 333.
[9] J. Studynka, B. Cechalova, V. Cech, Surf. Coat. Technol. 202 (2008) 5505.
[10] G.E. Jellison Jr., F.A. Modine, Appl. Phys. Lett. 69 (1996) 371.
[11] W.C. Oliver, G.M. Pharr, J. Mater. Res. 7 (1992) 1564.
[12] L. Martinu, J.E. Klemberg-Sapieha, O.M. Kuttel, A. Raveh, M.R. Wertheimer, J. Vac. Sci. Technol. A 12 (1994) 1360.
[13] V. Cech, J. Studynka, B. Cechalova, J. Mistrik, J. Zemek, Surf. Coat. Technol. 202 (2008) 5572.
[14] D.A.G. Bruggeman, Ann. Phys. 24 (1935) 636.
[15] V. Cech, J. Studynka, N. Conte, V. Perina, Surf. Coat. Technol 201 (2007) 5512.
[16] B.S. Mitchell, Materials Engineering and Science for Chemical and Materials Engineers, Wiley-Interscience, New Jersey, 2004, p. 851.
[17] E.A. Irene, In: H.G. Tompkins, E.A. Irene (Eds.), Handbook of Ellipsometry, William Andrew/Springer, Norwich, 2005, p. 573.